Statistical tests for the detection of intermediate structure: Application to the structure of the ^{238}U neutron capture cross section between 5 keV and 0.1 MeV

R. B. Perez, G. de Saussure, R. L. Macklin, and J. Halperin
Oak Ridge National Laboratory, Oak Ridge, Tennessee 37830
(Received 20 October 1978)

Recent measurements of the ^{238}U neutron capture cross section show a considerable amount of fluctuation between 5 and 100 keV. Statistical tests performed on the measured cross section suggest that the fluctuations are not compatible with the statistical model of nuclear reactions and imply the existence of intermediate structure, which is interpreted in terms of doorway states. The validity of the statistical tests used here is confirmed by numerical experiments with simulated cross sections generated by the Monte Carlo method, in accordance with the statistical method. The behavior of the capture cross section is compared to those of the subthreshold fission cross section and of the inelastic scattering cross section. The threshold anomaly at the opening of the inelastic channel at 45 keV is seen in the form of a rounded step.

[NUCLEAR REACTIONS Neutron capture ^{238}U(n,γ). E = 5 keV – 0.1 MeV measured $\sigma(E)$; statistical tests for intermediate structure; doorway states.]

I. INTRODUCTION

There is a considerable amount of evidence establishing the existence of marked fluctuations in the ^{238}U(n,γ) cross section in the unresolved resonance region.[1,2] Similar fluctuations have also been reported in the ^{238}U total cross section, at somewhat higher energies.[3] These fluctuations are wider than the sharp resonances associated with the compound nucleus levels and narrower than the broad structure due to the energy dependence of the neutron penetration coefficients. They represent departures from the statistical nuclear model in localized energy regions, forming an intermediate structure which is not predicted by the compound nucleus theory.

There is some uncertainty[1] as to the overall shape of the ^{238}U(n,γ) cross section. In particular the two measurements discussed here differ by as much as 7% in the 20- to 100-keV region. However, a consistent pattern of cross-section fluctuations, with which this work is concerned, is observed in these measurements, as illustrated in Figs. 1, 2, and 3.

In Fig. 1 the results of two measurements discussed in Sec. II are compared to an optical model calculation by Jary *et al.*[4] The two measurements used neutrons produced with the Oak Ridge Electron Linear Accelerator (ORELA) but very different capture detectors. The data shown on Fig. 1 have been averaged in 1-keV wide intervals. The same data averaged over 400-eV wide intervals are also compared in Fig. 3. In Fig. 2 the data from one of the measurements discussed in Sec. II are compared to the results of a measurement by Spencer and Käppeler[2] using neutrons produced with the Kernforschungszentrum Karlsruhe (KFK) 3 MeV Van de Graaff accelerator.

Statistical tests[5,6] were performed on the measured cross sections to determine if the fluctuations are consistent with the statistical model of nuclear reactions or imply the existence of intermediate structure.[7-10] The interpretation

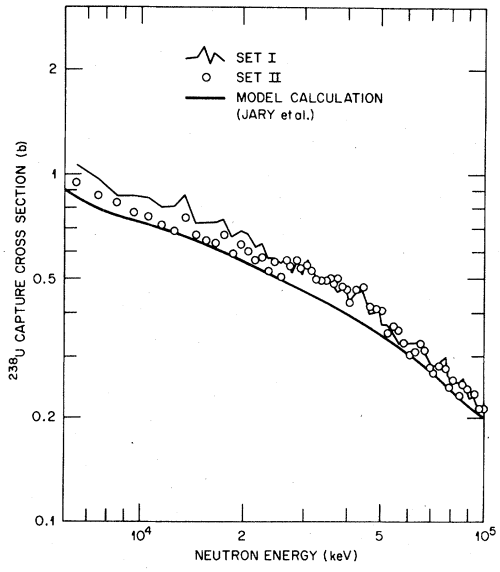

FIG. 1. Comparison of two sets of experimental ^{238}U capture cross sections with the model calculation of Jary *et al.*,[4] for neutron energies between 6 keV and 100 keV.

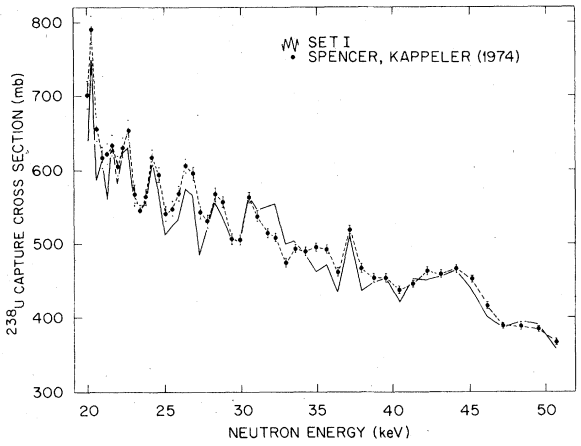

FIG. 2. Comparison of data set I with the ^{238}U capture cross-section measurement of Spencer and Käppeler[2] for neutron energies between 20 keV and 50 keV.

of the results of these statistical tests was first validated by applying these same tests to simulated cross sections.

In Sec. II we give a brief description of the $^{238}U(n,\gamma)$ cross-section measurements utilized in this work; a fit to the average cross section is discussed in Sec. III, in particular the threshold anomaly at the opening of the inelastic channel at 45 keV is seen in the form of a rounded step. In Sec. IV an interpretation of the observed intermediate structure in terms of doorway states is proposed. The statistical tests performed on the measured cross sections and their validation with simulated data are discussed in the last few sections.

II. THE $^{238}U(n,\gamma)$ CROSS-SECTION MEASUREMENTS

In this section we give a very brief description of the experimental techniques used in obtaining the two sets of data utilized in this work: sets I and II. More complete descriptions of the measurements, of the experimental techniques, and of the apparatus have been published elsewhere.[1,11]

Both measurements were done by the time-of-flight technique at the neutron time-of-flight facility associated with the pulsed electron accelerator ORELA. Table I gives the relevant parameters for both experiments. In each case the efficiency of the capture γ ray detector was obtained by the application of the saturated resonance method[1] to the ^{238}U resonance at 6.7 eV.

For data set I the detector was a large liquid scintillator surrounding a centrally located ^{238}U metallic sample. This scintillator was traversed by an aluminum tube through which the collimated neutron beam passed and in which the ^{238}U sample was placed, normal to the neutron beam. This detector was large enough to absorb most of the

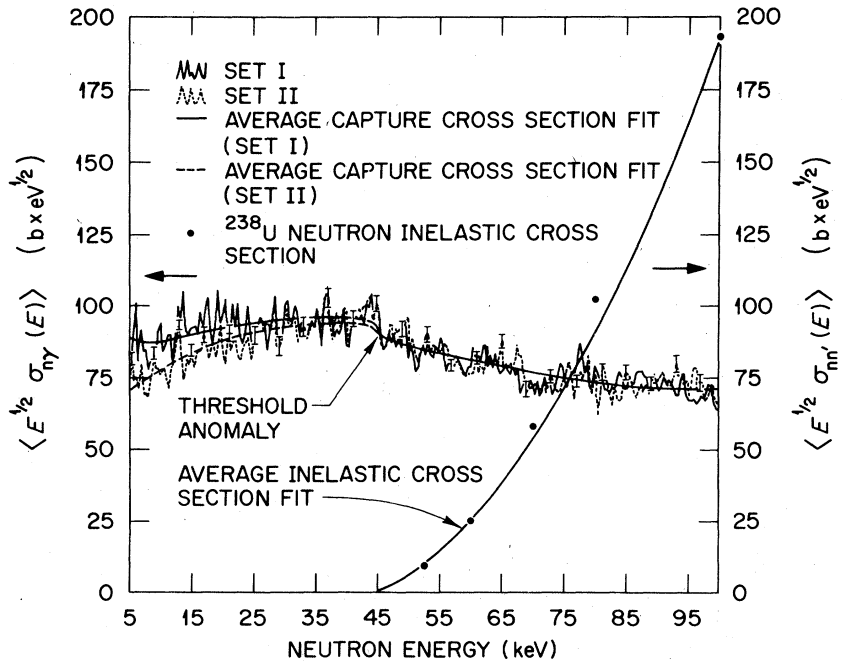

FIG. 3. The ^{238}U capture cross section averaged over neutron energy intervals 400-eV wide for sets I and II. Also shown in the figure are the average cross-section fits to both sets of data and the average cross-section fit to the ^{238}U neutron inelastic cross section. The statistical error bars are shown at selected points to avoid excessive cluttering.

TABLE I. Experimental parameters for the $^{238}U(n,\gamma)$ cross-section measurement for set I and set II.

	Set I	Set II
Linac repetition rate (Hz)	450	800
Electron burst width (ns)	5	5
^{238}U sample thickness (atoms/barn)	0.0028	0.0028
Flight-path length (m)	39.70	40.09

γ rays emitted by the sample so that the detection efficiency was a function of the total emitted photon energy (i.e., binding energy plus center-of-mass neutron energy), and was fairly insensitive to the multiplicity of the capture γ ray cascade.

For data set II the detector consisted of two symmetrically located nonhydrogenous scintillation counters viewing a metallic ^{238}U sample placed normal to the neutron beam. For each event the digital output of this system was on-line processed by application of a pulse-height weighting scheme resulting in a weighted response proportional to the total emitted photon energy.

The shape of the incident neutron spectrum was obtained with a $^{10}BF_3$ ionization chamber for set I, and with a ^6Li glass detector[12] for set II.

As previously stated there is a shape difference between the two data sets resulting in a 7% difference between 20 and 100 keV. For the analysis presented here the data of set I were renormalized to those of set II in the region 20 to 100 keV.

Sets I and II are compared in Figs. 1, 3, and 4. In Fig. 1 the data are averaged over 1-keV intervals and compared to an optical model calculation of Jary *et al.*[4] In Fig. 3 the data are averaged over 400-eV intervals; the statistical error is indicated at a few selected points. This figure also shows the inelastic scattering cross section and fits to the data which will be discussed in Sec. III. In Fig. 4 the data are averaged over 10-keV wide intervals: the fluctuations due to intermediate structure have been "washed out" by the averaging and the only remaining feature is a "rounded step" at the opening of the first inelastic threshold.[13]

III. THE AVERAGE CROSS-SECTION FIT AND THRESHOLD EFFECTS

In this section we discuss a fit to the data averaged over wide energy intervals. This fit is intended to represent the long-range behavior of the cross sections, averaged over any intermediate structure which may exist; the results of the fit will be used as a "reference line" for the Wald-Wolfowitz runs tests to be described in Secs. V and VI. In the neutron energy range considered here, an inelastic neutron channel opens at 45 keV due to the 2+ state in the ^{238}U nucleus. The data (see Figs. 3 and 4) exhibit a threshold anomaly which appears as a rounded step[13] rather than as a Wigner cusp shape.[14] It has been shown[14,15] that for neutral particles, the threshold anomaly can be described in terms of a power series in the wave number, i.e., $\sigma_{n\gamma}^{(l)} \sim k^{2l+1}$, where l is the angular momentum in the channel. Because of the unitarity property of the collision matrix the threshold effects affect all the reaction channels above and below the threshold energy. In order to describe the opening of the inelastic channel, a simultaneous fit to the capture data and to an evaluation of the inelastic neutron cross section[16] was performed. The average capture and inelastic cross sections[17] $\sigma_{n\gamma}(E)$ and $\sigma_{nn'}(E)$ are given for a specified (J,l) contribution by:

$$\langle E^{1/2}\sigma_{n\gamma}^{(J,l)}\rangle = \sigma_0 g_J V_l \frac{\langle\Gamma_\gamma^{(l)}\rangle}{\langle\Gamma^{(J,l)}\rangle} S_{0l}^J R_l^{n\gamma} + \mathrm{sgn}(E-E_c)a_l\rho_0^{2l+1}, \quad (1)$$

$$\langle E^{1/2}\sigma_{nn'}^{(J,l)}\rangle = \sigma_0 g_J V_l' \frac{\langle\Gamma_{n'}^{(J,l)}\rangle}{\langle\Gamma^{(J,l)}\rangle} S_{0l}^J R_l^{nn'\gamma} + b_l\rho_0^{2l+1}, \quad (2)$$

where the penetration factors V_l and V_l' as well as the fluctuation factors[18] $R_l^{n\gamma}$ and $R_l^{nn'\gamma}$ are defined in Appendix A. We also have

$$\sigma_0 = 4.125\times10^6 \ (\mathrm{b\,eV^{1/2}}),$$

and

$$g_J = \text{spin statistical weight factor} = \frac{2J+1}{2(2I+1)},$$

where I is the spin of the target nucleus and J the total angular momentum.

The total angular momentum dependent strength functions, S_{0l}^J, are defined in the form

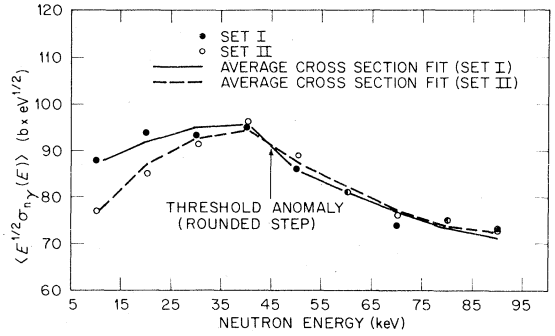

FIG. 4. The ^{238}U neutron capture cross section of sets I and II, averaged over neutron energy intervals 10-keV wide, for neutron energies between 5 keV and 0.1 MeV.

TABLE II. Average resonance parameters for the average cross-section calculation.

l	J	g_J	$D^{(J,l)}$ [a] (eV)	$\langle\Gamma_{0n}^{(J,l)}\rangle$ [a,b,c] (eV)
0	$\frac{1}{2}$	1	24.8	0.002 88
1	$\frac{1}{2}$	1	26.73	0.005 2
1	$\frac{3}{2}$	2	13.37	0.002 6
2	$\frac{3}{2}$	2	12.40	0.001 44
2	$\frac{5}{2}$	3	8.30	0.000 96

[a] Data from Ref. 39.
[b] Reduced widths.
[c] The average capture width $\langle\Gamma_\gamma\rangle$ was taken to be 0.0235 eV (see Ref. 39).

$$S_{0l}^{J}=\frac{\langle\Gamma_{0n}^{(J,l)}\rangle}{\langle D^{(J,l)}\rangle}, \tag{3}$$

where $\langle\Gamma_{0n}^{(J,l)}\rangle$ is the average reduced neutron width and $\langle D^{(J,l)}\rangle$ is the average level spacing. The calculation of the partial widths $\langle\Gamma_{n}^{(J,l)}\rangle$ (neutron width) and $\langle\Gamma_{n'}^{(J,l)}\rangle$ (inelastic neutron width) is described in Appendix A. The input parameters for the average cross-section calculation are shown in Table II. The quantity ρ_0 is defined as: (see Appendix A for units and definitions)

$$\rho_0=(2.19\times10^{9})(|E-E_c|)^{1/2}a, \tag{4}$$

where E is the neutron energy (eV) and a is the channel radius, in cm. Starting from the values of the strength functions computed from the input data in Table II as initial guesses the parameters varied in the simultaneous fits are the strength functions, S_{0l}^{J}, the inelastic neutron widths, $\Gamma_{n'}^{(J,l)}$, and the coefficients, a_l and b_l. The parameters a_l and b_l which mockup the rounded step anomaly are not strictly independent as they are related by the unitarity of the collision matrix. The unitarity constraint is violated by varying them independently in the fitting procedure over a limited energy range. In consequence the average cross-section fit so obtained is only an approximate representation of the cross section in the energy range considered

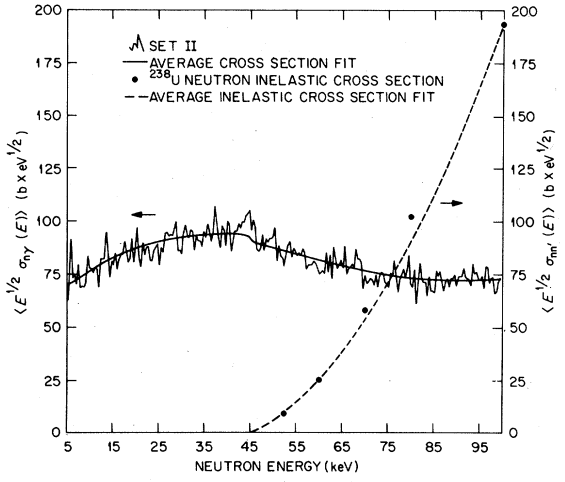

FIG. 5. The ^{238}U neutron capture cross section for set II averaged over neutron energy intervals 400-eV wide for neutron energies between 5 keV and 0.1 MeV. Also shown in the figure are the average neutron capture and inelastic average cross-section fits as well as the evaluation (Ref. 16) of the neutron inelastic cross section.

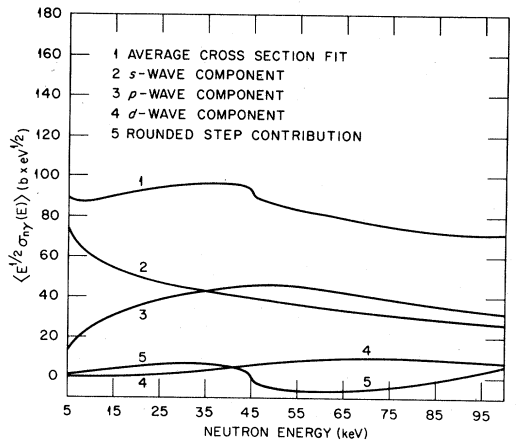

FIG. 6. The average neutron capture cross section fit to set I for neutron energies between 5 keV and 0.1 MeV. Also shown in the figure are the s-wave, p-wave, d-wave, and rounded step contributions to the total average capture fit.

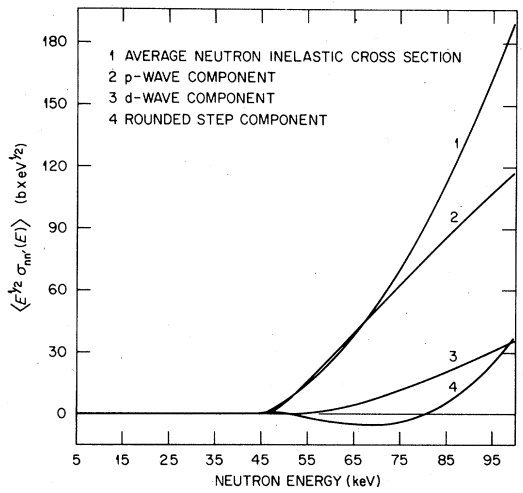

FIG. 7. The average neutron inelastic cross section fit to set I for neutron energies between 5 keV and 0.1 MeV. Also shown in the figure are the p-wave, d-wave, and rounded step contributions to the total average inelastic fit.

in this work. The results of the simultaneous fits are shown for set I and set II in Figs. 3 and 5, respectively. The s-wave, p-wave, and d-wave contributions to the average cross-section fit to set I are shown in Fig. 6 together with the contribution arising from the rounded step. The p-wave and d-wave components of the average inelastic neutron cross section as well as the threshold contributions are shown in Fig. 7 for set I.

The strength functions, inelastic widths, and "cusp" coefficients obtained from the simultaneous fits are given in Tables III and IV for set I and set II, respectively. The difference between the strength functions and inelastic threshold parameters for both data sets is a reflection of the difference in shape between the measurements.

IV. THEORETICAL INTERPRETATION OF THE INTERMEDIATE STRUCTURE IN NEUTRON REACTION CROSS SECTIONS

Current thoughts on the interpretation of intermediate structure are based on the concept of doorway states[19] which are "simple" states with a decay width to the continuum. A generalization of this concept was evolved by Lane[20] and Robson[21] by the introduction of "special states" with the following properties[20]:

(i) Their level widths are larger than the average width of the compound nucleus states.

(ii) They are not eigenfunctions of the total nuclear Hamiltonian, but of a slightly different Hamiltonian which differs from the former by a residual interaction.

(iii) They satisfy the boundary conditions of R-matrix theory.

The introduction of the special levels provides a particularly simple device to interpret the intermediate structure. Endowed with a large width and with a residual interaction potential, they interact with the compound nucleus levels, which share the strength of the special state. This process leads to enhancements of the cross section in localized energy regions which cannot be explained in the framework of the statistical nuclear model.

Special states can exist both at the entrance channel and at the exit channel of a nuclear reaction. The entrance doorway states are responsible for the analog resonances observed in many nuclei (Robson[22]). Exit special states arising from

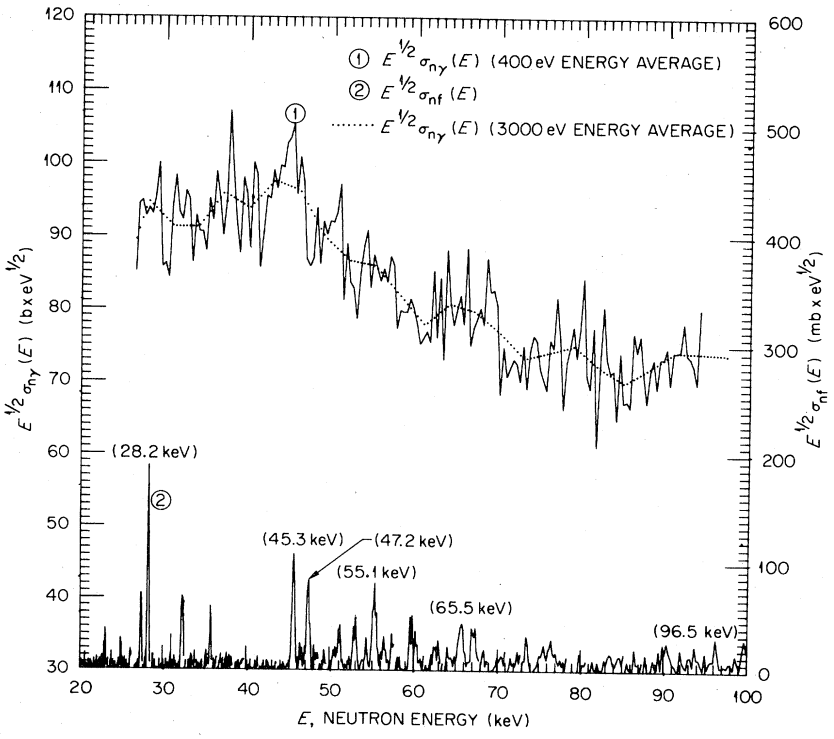

FIG. 8. Comparison between the ^{238}U neutron capture and subthreshold fission cross sections for neutron energies between 20 keV and 0.1 MeV.

the structure of the fission barrier at large nuclear deformations are responsible for the subthreshold fission structures.[23-25,20] The ^{238}U nucleus is known to have subthreshold fission structures.[26-29] Because of unitarity, the ^{238}U(n,γ) cross section could also show structures correlated to the threshold fission peaks. In Fig. 8 we have plotted the data set II averaged over 400-eV and 3-keV wide energy intervals and the ^{238}U neutron subthreshold fission cross section as measured by Difilippo *et al.*[28] There is an enhancement of the subthreshold fission cross section above the opening of the inelastic channel at 45 keV. However, because the fission cross section is very small compared with the magnitude of the fluctuations observed in the capture cross section, we shall attempt to describe the observed ^{238}U(n,γ) cross-section fluctuations in terms of the intermediate structure arising from the presence of entrance doorway states.

We have shown for a more general case[9] that in the presence of intermediate structure the average cross section for a given (J,Π,l) combination is given by the expression

$$\langle E^{1/2}\sigma_{n,\gamma}^{(J,l)}(E)\rangle = \sigma_1 E^{-1/2}\frac{\langle\Gamma_{\lambda\gamma}\rangle}{\langle\Gamma_\lambda\rangle}S_{n,\gamma}^{(J,l)}(E), \tag{5}$$

where

$$\sigma_1 = 2\pi^2\left(\frac{\hbar^2}{2M_c}\right)g_J, \tag{6}$$

and $S_{n,\gamma}^{(J,l)}(E)$ is a generalized strength function

$$S_{n,\gamma}^{(J,l)}(E) = S_n^{(J,l)}M_{n\gamma}^{(l)}(E). \tag{7}$$

The modulation factor $M_{n\gamma}^{(l)}(E)$ is given by

$$M_{n\gamma}^{(l)}(E) = [R_{1l} + R_{2l}\langle\theta_{\lambda,n}\rangle/S_n]/[1+\langle\phi_\lambda\rangle/\langle\Gamma_\lambda\rangle], \tag{8}$$

where

$$S_n^{(J,l)} = \langle\Gamma_{\lambda n}^{(J,l)}\rangle/\langle D_\lambda^{(J,l)}\rangle, \tag{9}$$

and $\langle D_\lambda^{(J,l)}\rangle$ is the average level spacing of the compound nucleus levels, while R_{1l} and R_{2l} are statistical fluctuation factors defined in Appendix A. The factors $\langle\theta_{\lambda,n}\rangle$ and $\langle\phi_\lambda\rangle$ are given in terms of the nuclear parameters of the doorway states and compound nucleus levels by the expressions

$$\langle\theta_{\lambda,n}\rangle = \sum_\mu |W_{0\mu}|^{-2}[\Gamma_\mu U_{\mu n} - K_{\mu n}(E_\mu - E)], \tag{10}$$

$$\langle\phi_\lambda\rangle = \sum_\mu |W_{0\mu}|^{-2}[\Gamma_\mu I_\mu - 2J_\mu(E_\mu - E)], \tag{11}$$

where the summations go over the doorway states. Both factors, $\langle\theta_{\lambda,n}\rangle$ and $\langle\phi_\lambda\rangle$, consist of the superposition of generalized Breit-Wigner resonances with asymmetric terms, depending on the energy of the doorway states. The energy denominators, $|W_{0\mu}|^2$, are given by

$$|W_{0\mu}|^2 = (E_\mu - E)^2 + \tfrac{1}{4}\Gamma_\mu{}^2, \tag{12}$$

where E_μ and Γ_μ are the doorway state energies and widths, respectively. In turn the symmetric factors $U_{\mu n}$ and I_μ and the asymmetric factors $K_{\mu n}$ and $J_{\mu n}$ are given by the expressions:

$$U_{\mu n} = \frac{1}{\Gamma_\mu}\langle\Gamma_\mu^\downarrow\rangle\Gamma_{\mu n} - 2\langle Y_{\mu\lambda n}^\downarrow\rangle, \tag{13}$$

$$I_\mu = \langle\tilde{V}_{\mu\lambda}{}^2\rangle - \tfrac{1}{4}\langle\Gamma_{\mu\lambda}{}^2\rangle, \tag{14}$$

$$K_{\mu n} = 2\langle\xi_{\mu\lambda n}^\downarrow\rangle, \tag{15}$$

$$J_\mu = \langle\tilde{V}_{\mu\lambda}\Gamma_{\mu\lambda}\rangle, \tag{16}$$

where the angular brackets indicate the ensemble average over the compound nucleus levels and where we introduced the following definitions:

$$\langle\Gamma_\mu^\downarrow\rangle = \text{average spreading width} = \langle(\tilde{V}_{\mu\lambda}{}^2 + \tfrac{1}{4}\Gamma_{\mu\lambda}{}^2)\rangle/\langle D_\lambda\rangle, \tag{17}$$

$$\langle Y_{\mu\lambda n}^\downarrow\rangle = \text{external mixing partial width} = \langle\Gamma_{\lambda n}\Gamma_{\mu n}\rangle^{1/2}(\langle\Gamma_{\mu\lambda}\rangle/\langle D_\lambda\rangle), \tag{18}$$

$$\langle\xi_{\mu\lambda n}^\downarrow\rangle = \text{internal mixing partial width} = \langle\Gamma_{\lambda n}\Gamma_{\mu n}\rangle^{1/2}(\tilde{V}_{\mu\lambda}/\langle D_\lambda\rangle). \tag{19}$$

Finally, the interaction matrix elements $\tilde{V}_{\mu\lambda}$ and interaction widths $\Gamma_{\mu\lambda}$ are defined as

$$\tilde{V}_{\mu\lambda} = \langle\mu|V_{\text{residual}}|\lambda\rangle - S_{\mu\lambda}, \tag{20}$$

$$\Gamma_{\mu\lambda} = \sum_c(\Gamma_{\mu c}\Gamma_{\lambda c})^{1/2}, \tag{21}$$

with

$$S_{\mu\lambda} = \sum_c S_c\gamma_{\mu c}\gamma_{\lambda c}. \tag{22}$$

The sums in Eqs. (21) and (22) go over all channels. S_c is the channel shift factor, $\Gamma_{\mu c}$ and $\Gamma_{\lambda c}$ are the partial level widths for the doorway states and compound nucleus states, respectively, and $\gamma_{\mu c}$ and $\gamma_{\lambda c}$ are the corresponding R-matrix reduced widths. The residual "force", (V_{residual}), arises from the fact that the doorway states are not eigenfunctions of the total nuclear Hamiltonian, as mentioned at the beginning of this section.

Following Lane's[20] conception of the special states, their interaction with the compound nucleus levels proceeds both by the residual force, V_{residual} (internal mixing), and by "level overlapping" (external mixing), the latter effect arising because the "special levels" satisfy the boundary conditions of the R matrix rather than the Kapur-Peierls boundary conditions associated

with the collision matrix. The external mixing appears through the interaction widths $\Gamma_{\mu\lambda}$ and the energy shift factors $S_{\mu\lambda}$. This effect accounts for the extra terms in our definition (Eq. 17) of the spreading width, and for the partial mixing width $Y^{\downarrow}_{\mu\lambda n}$. The external mixing also accounts for the asymmetric factor J_μ. The inclusion of the external mixing is a reflection of the physical fact that the level overlap, together with the residual interaction, determines the strength of the intermediate structure.

The average external and internal partial widths $\langle Y^{\downarrow}_{\mu\lambda n}\rangle$ and $\langle \xi^{\downarrow}_{\mu\lambda n}\rangle$ depend on the covariance between the compound nucleus level neutron width $\Gamma^{1/2}_{\lambda n}$ and the width of the doorway state. The symmetric factor $U_{\mu n}$ has a "direct" term, proportional to the average spreading width, and an interference term controlled by the average external partial mixing width $\langle Y^{\downarrow}_{\mu\lambda n}\rangle$. The symmetric factor I_μ depends on the balance between the second moments of the distribution of the interaction elements $\tilde{V}_{\mu\lambda}$ and $\Gamma_{\mu\lambda}$. The asymmetric factor $K_{\mu n}$ is proportional to the average internal partial width $\langle \xi^{\downarrow}_{\mu\lambda n}\rangle$, whereas J_μ is just the covariance between $\tilde{V}_{\mu\lambda}$ and $\Gamma_{\mu\lambda}$. Hence a fit of the expression (5) [where the parameters, Γ_μ, $U_{\mu n}$, $K_{\mu n}$, I_μ, and J_μ, in Eqs. (10) and (11) are to be varied] to the intermediate structure data, will yield information on statistical parameters such as averages, second moments, and covariances of the nuclear parameters of the interaction between the doorway states and the compound nucleus levels. However, the most interesting feature of the present model is that of providing an explanation for the enhancements of the capture cross section, in the energy regions around the doorway states.

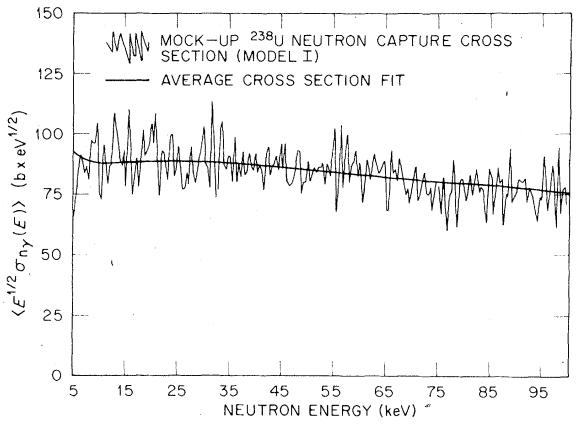

FIG. 9. The mockup ^{238}U neutron capture cross section (model I), constructed in accordance with the statistical nuclear model. The smooth solid line is the average cross section fit (s-wave and p-wave contributions). The simulated cross-section data have been averaged over neutron energy intervals 400-eV wide for neutron energies between 5 keV and 0.1 MeV.

V. STATISTICAL TESTS FOR THE DETECTION OF INTERMEDIATE STRUCTURE

The problem of extracting the intermediate structure from the fluctuations in the cross section arising from the superposition of many compound nucleus resonances has been extensively studied.[6,30-32] Recently James[10] applied the Wald-Wolfowitz[5] distribution-free statistics to the detection of intermediate structure in the fission cross section of several nuclei.[30]

The Wald-Wolfowitz runs test deals with the number of runs, R, of consecutive values which lie above or below a given reference line. The Wald-Wolfowitz statistics provide the number of runs, $E(R)$, expected from random statistical data, as well as the standard deviation $\sigma(R)$. It can be shown that the ratio

$$\epsilon_R = \frac{|R - E(R)| - \frac{1}{2}}{\sigma(R)} \tag{23}$$

approximates a normal probability distribution.

To apply the runs tests, the data were first binned into 10-keV wide intervals so as to average over the cross-section fluctuations. A cross-section fit was then performed, as described in the previous section. This fit reproduces accurately the long-range behavior of the data (see Fig. 4) and was used as the reference line for the runs test performed with the same data binned over intervals of width Δ, smaller than the width of the fluctuations but larger than the average widths of the compound nucleus levels and of the experimental resolution function.

The autocorrelation function of the capture cross section was also investigated to determine if the data exhibited correlations longer than those

TABLE III. Average parameters from the simultaneous fit of the ^{238}U average neutron capture and inelastic cross sections for data set I (threshold effects included).

l	J	$S_{0_l}(\times 10^{-4})$	$\Gamma^{(J,l)\,a}_{0_n}$ (eV)	a_l (b eV$^{1/2}$)	b_l (b eV$^{1/2}$)
0	$\frac{1}{2}$	1.285		34.3	11.0
1	$\frac{1}{2}$	0.936	0.002 42	−386	−1283
1	$\frac{3}{2}$		0.001 21	−386	−1283
2	$\frac{3}{2}$	0.051	0.120 7	843	8372
2	$\frac{5}{2}$		0.080 5	843	8372

[a] Reduced widths.

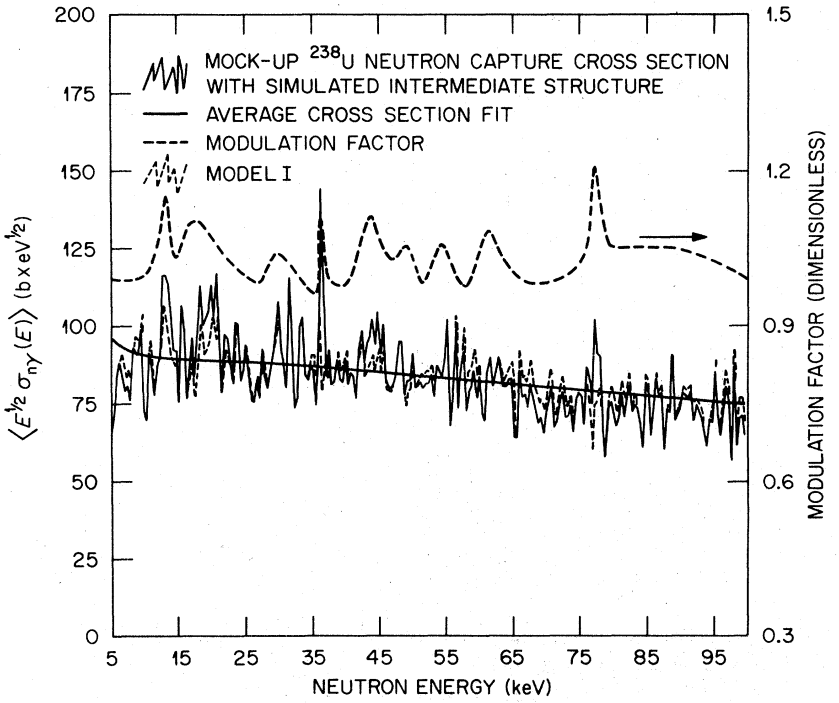

FIG. 10. The ^{238}U mockup capture cross sections with and without intermediate structure (model II and model I, respectively). Also shown in this figure is the modulation factor introduced in the nuclear statistical model to simulate the intermediate structure. The data shown have been averaged over neutron energy intervals 400-eV wide between 5 keV and 0.1 MeV.

expected from the widths of the resonances of the compound nucleus and of the resolution function of the measurements.

To evaluate the ability of the runs test and of the autocorrelation function to detect intermediate

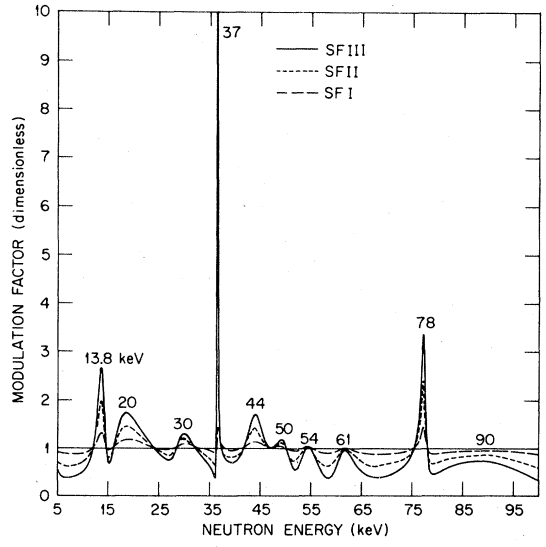

FIG. 11. The various modulation factors, S.I, S.II, and S.III used (see Sec. V) for the simulation of mockup cross sections with intermediate structure (model II, model III, and model IV, respectively).

structure, studies were done with a simulated ^{238}U capture cross section generated in accordance with the statistical model of the compound nucleus.

To approach a realistic situation, the mockup cross sections must exhibit, besides the fluctuations arising from the statistics of the resonance parameters, the experimental resolution broadening and "background" due to "faraway" levels, since the latter two effects contribute to the energy correlations within the data set. The procedure followed was to divide the neutron energy region between 5 and 100 keV into intervals 100-eV wide. The choice of this interval was based on the fact that the experimental energy resolution in this energy range is 100 eV on the average. Neglecting level interference effects,[33] the cross section for a given angular momentum component, l, is well described by the superposition of Breit-Wigner resonances, i.e.,

$$E^{1/2}\sigma_{n,\gamma}(E) = \sigma_1 \sum_\lambda \frac{\langle\Gamma_\gamma\rangle \Gamma_{n\lambda}^{(l)}(E)}{(E-E_\lambda)^2 + [\frac{1}{2}\Gamma_\lambda^{(l)}(E)]^2}, \tag{24}$$

where σ_1 is a constant (see Eq. 6) and $\langle\Gamma_\gamma\rangle$ the average radiation width. We now define the average cross section

$$\langle E_i^{1/2}\sigma_{n\gamma}^{(l)}(E_i)\rangle = \frac{1}{\Delta}\int_{E_i-\Delta/2}^{E_i+\Delta/2} E^{1/2}\sigma_{n,\gamma}^{(l)}(E)\,dE, \tag{25}$$

TABLE IV. Average parameters from the simultaneous fit of the ^{238}U average neutron capture and inelastic cross sections for the data set II (threshold effects included).

l	J	S_{0_l} ($\times 10^{-4}$)	$\Gamma_{0n'}^{(J,l)}$ [a] (eV)	a_l (b eV$^{1/2}$)	b_l (b eV$^{1/2}$)
0	$\frac{1}{2}$	0.563		16.0	4.3
1	$\frac{1}{2}$	1.1	0.002 42	−270	−1624
1	$\frac{3}{2}$		0.001 21	−270	−1624
2	$\frac{3}{2}$	0.022	0.120 7	−513	9521
2	$\frac{5}{2}$		0.080 5	−513	9521

[a] Reduced widths.

to obtain

$$\langle E_i^{1/2}\sigma_{n\gamma}^{(l)}(E_i)\rangle = \frac{2\sigma_\perp}{\Delta}\langle\Gamma_\gamma\rangle\left\{\sum_\lambda [\Gamma_{n\lambda}^{(l)}(E_i)/\Gamma_\lambda^{(l)}(E_i)]G_\lambda(E_i)\right\}, \quad (26)$$

with

$$G_\lambda(E_i) = \tan^{-1}\left[\frac{E_i + \Delta/2 - E_\lambda}{\frac{1}{2}\Gamma_\lambda^{(l)}(E_i)}\right] - \tan^{-1}\left[\frac{E_i - \Delta/2 - E_\lambda}{\frac{1}{2}\Gamma_\lambda^{(l)}(E_i)}\right], \quad (27)$$

and where we neglected the energy dependence of the neutron widths within the interval of integration.[34] With $\Delta = 100$ eV, the program POLLA[35] was utilized for the generation of parameters from the appropriate Porter-Thomas[36] distributions, and for the generation of level spacings from the Wigner distribution law,[37] by the Monte Carlo techniques utilizing the average parameters in Table II. The effect of faraway levels was described by enlarging the energy range below 5 keV and above 100 keV by several average level spacings. The result of this calculation for the superposition of s-wave and p-wave components is shown in Fig. 9, where the solid line is the average cross-section fit described in Sec. III. (The rounded step contribution was not included in the generation of the mockup cross section.)

To simulate the effects of intermediate structure, the cross section computed according to the statistical nuclear model (model I) was modified by introducing in the $J = \frac{1}{2}$, $l = 1$ component, a modulation factor computed from Eq. (8) and the parameters in Table VIII, obtained from the fit of this equation to the capture data of set I, (see Sec. VII). The resulting modulation factor, S.I, and the corresponding simulated cross section are shown in Fig. 10. The modulation factor, S.I, fluctuates around unity, with broad asymmetric resonances around the location of the surmised doorway states. To study the runs test and the autocorrelation as a function of the amount of intermediate structure, two more sets of simulated cross sections, model III and model IV, were implemented with modulation factors, S.II $= 3(S.I - 1) + 1$, and S.III $= 5(S.I - 1) + 1$, respectively. The modulation factors, S.I, S.II, and S.III are shown in Fig. 11.

The results of the Wald-Wolfowitz Runs Test for the mockup capture cross sections, without the intermediate structure (model I) and with the modulation factor included (model II), are shown in Table V for energy averages of the cross section ranging from 200 eV up to 10 keV. The results pertaining to model I show that on the average there is a 27% probability of obtaining larger or equal ratios, ϵ_R, from a sample of random data. In the presence of intermediate structure this figure goes down to about 3% for values of the energy averaging interval, Δ, between 0.2 keV and 2 keV. For larger intervals the probability $P(\epsilon_R)$ increases again, indicating a progressive washout of the intermediate structure. Hence

TABLE V. Results of the Wald-Wolfowitz runs test for the mockup ^{238}U capture cross section with and without intermediate structure.

Δ [a] (keV)	Model I [b] ϵ_R	Model I [b] $P(\epsilon_R)$ (%)	Model II [c] ϵ_R	Model II [c] $P(\epsilon_R)$ (%)
0.2	0.30	38.0	2.20	1.4
0.4	0.74	23.0	3.41	0.03
1.0	0.09	46.0	1.37	8.0
2.0	0.89	18.0	2.49	0.65
3.0	1.08	14.0	1.05	14.7
10.0	0.68	25.0	1.41	7.8

[a] Energy averaging interval.
[b] Mockup cross section without intermediate structure.
[c] Mockup cross section with intermediate structure.

TABLE VI. Results of the Wald-Wolfowitz runs test for various mockup ^{238}U neutron capture cross sections with simulated intermediate structure.

Δ (eV)	Model II [a] ϵ_R	Model II [a] $P(\epsilon_R)$ (%)	Model III [a] ϵ_R	Model III [a] $P(\epsilon_R)$ (%)	Model IV [a] ϵ_R	Model IV [a] $P(\epsilon_R)$ (%)
200	2.20	1.4	10.00	$<10^{-15}$	13.49	$<10^{-15}$
400	3.41	0.03	9.10	$<10^{-15}$	11.66	$<10^{-15}$

[a] Model II consists of the mockup ^{238}U capture cross section modulated by the intermediate structure extracted from the experimental data (see Sec. VII). Models III and IV are described in Sec. V.

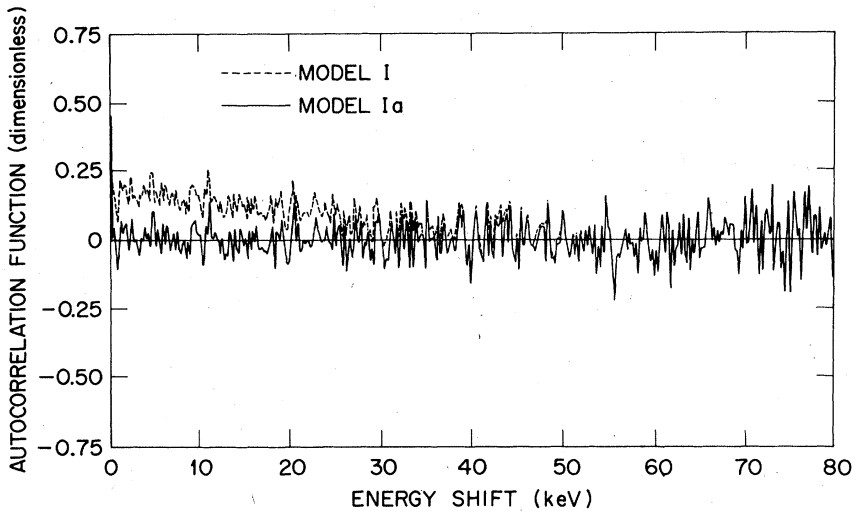

FIG. 12. Autocorrelation functions for the simulated ^{238}U neutron capture cross section, model I and for model I.a, which is the result of subtracting the average cross-section fit from model I. The simulated cross sections have been averaged over neutron energy intervals 200-eV wide.

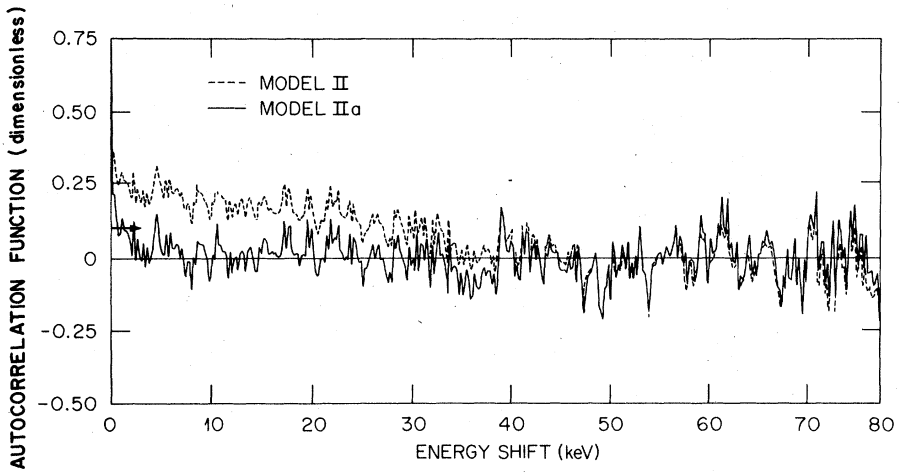

FIG. 13. Autocorrelation functions for simulated ^{238}U neutron capture cross section with intermediate structure, model II, and for model II.a, which is the result of subtracting the average cross-section fit from model II. The simulated cross sections have been averaged over neutron energy intervals 200-eV wide.

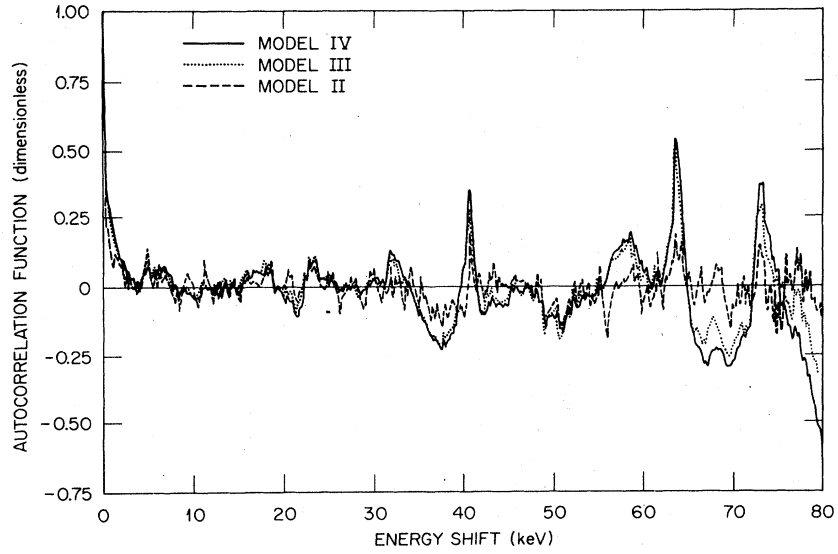

FIG. 14. Autocorrelation functions for the simulated ^{238}U neutron capture cross sections, model II.a, model III.a, and model IV.a. These simulated cross sections are obtained by subtraction of the average cross-section fit from model II, model III, and model IV, respectively. The simulated cross sections have been averaged over neutron energy intervals 200-eV wide.

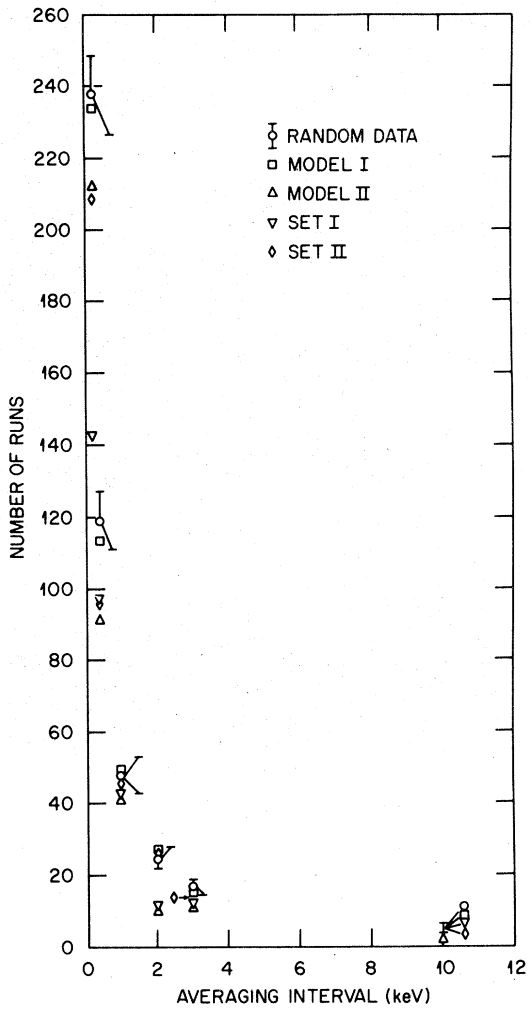

FIG. 15. The Wald-Wolfowitz runs test for various simulated ^{238}U neutron capture cross sections and the experimental data, compared with the expected number of runs from a set of randomly distributed objects.

for the particular intermediate structure introduced in the data the Wald-Wolfowitz runs test indicates the persistency of intermediate structure effects up to energy intervals as wide as 3 keV. For the 400-eV capture cross section averages, there is a factor of five increase in the ratio, ϵ_R, for the model II case.

The results of the Wald-Wolfowitz runs test for Models II, III, and IV are shown in Table VI for $\Delta = 200$ eV and 400 eV. These results show the sensitivity of the runs test to the amount of intermediate structure.

The autocorrelation function tests (see Appendix A) are displayed in Figs. 12, 13, and 14. In Fig. 12 we show the autocorrelation functions for model I and model I.a, for the simulated cross sections averaged over 200-eV intervals. In the case of the simulated cross section (model I), there is a correlation range of about 40 keV. Beyond this range the autocorrelation function oscillates around its zero value. Upon subtraction of the average cross-section fit (see Sec. III), from the mockup cross section, the resulting data set (model I.a) gives an autocorrelation function with a correlation range of only 200 eV, which arises from the "box" averaging of the data. We then conclude that the 40-keV correlation range exhibited in the case of model I is due to the energy dependence of the neutron penetration coefficients. The autocorrelation functions for the simulated cross section with intermediate structure (model II), and for the result of subtracting the average cross section fit from model II (i.e., model II.a), are shown in Fig. 13. After thus "peeling off" the energy dependence of the neutron penetration coefficients, there appears to be a short correlation range of about 3 keV followed by various correlation peaks. These peaks arise whenever there is a coincidence between two peaks in the cross section at given energy shifts. This feature is clearly seen in Fig. 14, which displays the autocorrelation functions for models II, III, and IV, after subtraction of their respective average cross-section fits. In this feature the large peak seen at 64 keV arises from the pair of peaks at 78 keV and 14 keV present in the modulation factor (see Fig. 11). With few exceptions, such as, for instance, the peak seen at an energy shift of about 75 keV, which seems to arise from end effects, most of the correlation peaks can be traced back to pairs of peaks in the modulation factor.

VI. STATISTICAL TESTING OF THE ^{238}U NEUTRON CAPTURE CROSS SECTION

In this section we apply the statistical tests discussed in the previous section to the two sets of capture data. The reference line appropriate to each set was subtracted from the data (averaged over 400-eV energy intervals). This operation separates out the fluctuations from the average behavior. Next the fluctuations obtained from set I were subtracted from the fluctuations in set II. The set of points resulting from this operation yielded a value for ϵ_R of 0.81. There is a probability of 21% for a value equal or larger than 0.81 to be obtained from a set of random objects. Hence the fluctuations remaining in set II, after subtracting the fluctuations in set I, appear to be random.

The Wald-Wolfowitz runs test was applied to data sets I and II for several values of the averaging energy interval Δ. Figure 15 shows the ex-

TABLE VII. Results of the Wald-Wolfowitz runs test for the ^{238}U capture cross-section measurements (sets I and II) and comparison with the results obtained for model II.

	Set I		Set II		Model II	
Δ [a] (keV)	ϵ_R	$P(\epsilon_R)$ (%)	ϵ_R	$P(\epsilon_R)$ (%)	ϵ_R	$P(\epsilon_R)$ (%)
0.2	8.72	$<10^{-15}$	2.65	0.4	2.20	1.4
0.4	2.81	0.2	2.99	0.1	3.41	0.03
1.0	1.03	15.0	0.42	33.0	1.37	8.0
2.0	2.34	0.9	0.30	38.0	2.49	0.65
3.0	0.98	16.0	0.36	36.0	1.05	14.7
10.0	0.4	34.0	0.40	34.0	1.41	7.8

[a] Energy averaging interval.

pected number of runs from a set of random objects with the corresponding standard deviation. Shown also in the figure are the runs obtained for the mockup cross sections, models I and II, as well as the corresponding runs for sets I and II. For $\Delta = 200$ eV up to 10 keV, the results for model I (i.e., the cross section computed according to the statistical nuclear model) fall within the error bands of the number of runs expected from a randomly distributed set of objects. For values of Δ up to 2 keV, model II as well as sets I and II show deviations from the random results. Above 3 keV, the number of runs obtained in each case falls within the error band of the random set of data. The ratios ϵ_R as well as the probability $P(\epsilon_R)$ obtained for each cross-section set are given in Table VII. These results indicate that the experimental cross section data behave in a manner similar to the data constructed on the basis of the statistical nuclear model modified by the inclusion of intermediate structure. For $\Delta = 400$ eV the significance level for the structure in the ^{238}U capture cross section is equal to that corresponding to about 3 standard deviations for a normal distribution.

The autocorrelation function for data set I averaged over 200-eV intervals is displayed in Fig. 16. As in the case of the mockup cross sections, there is a correlation range of about 40 keV. After peeling off the long-range correlation due to the energy dependence of the neutron penetration, the autocorrelation function is qualitatively similar to the autocorrelation function of the mockup capture data with the simulated intermediate structure. The same structure is observed for the autocorrelation function for set I averaged over 400-eV energy intervals (Fig. 17). As in the case of the simulated cross section

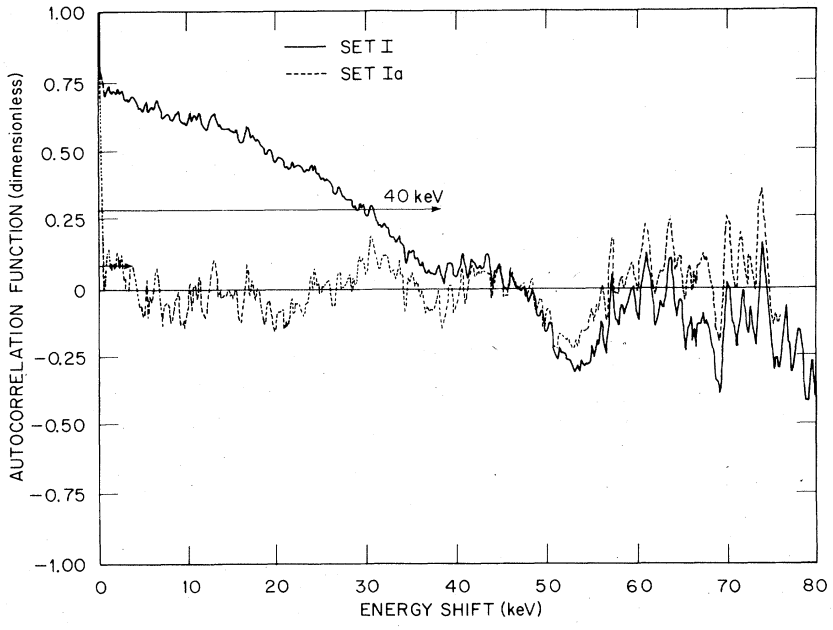

FIG. 16. Autocorrelation functions for set I and for set I.a obtained from set I by subtracting the average cross-section fit. The cross-section data have been averaged over neutron energy intervals 200-eV wide.

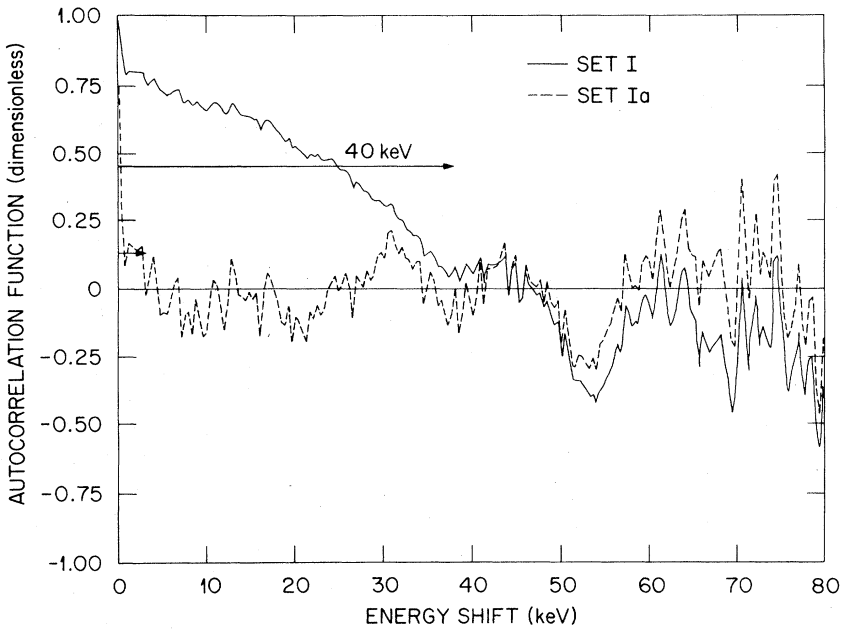

FIG. 17. Autocorrelation functions for set I and for set I.a obtained from set I by subtracting the average cross-section fit. The cross-section data have been averaged over neutron energy intervals 400-eV wide.

with intermediate structure, a correlation range of around 3 keV appears in the autocorrelation function for the experimental data. One could, in principle, surmise that this feature is related to the presence of some characteristic correlation width associated with the intermediate structure.

The cross correlation function between set I and set II, averaged over 400-eV energy intervals, is shown in Fig. 18. In the event of complete consistency between the data, the cross correlation function should coincide with the autocorrelation functions for set I and set II.

The resulting cross correlation function is consistent with the autocorrelation of set I after subtraction of the average cross-section fit, which reflects the reproducibility of the intermediate structure between set I and set II.

The Wald-Wolfowitz runs test, as well as the autocorrelation function test applied on the experimental data, are consistent with similar tests on the mockup cross sections. On the basis of this comparison, we surmise the presence of

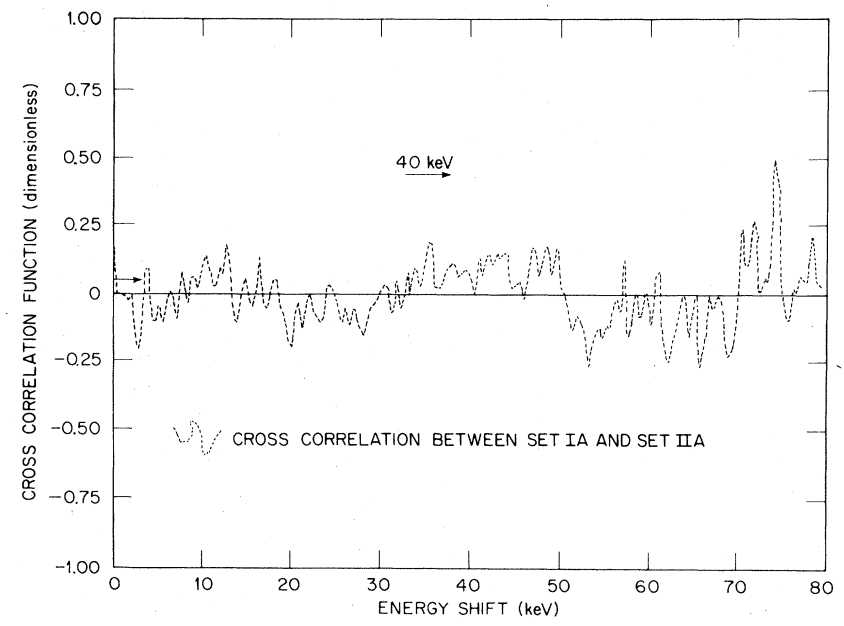

FIG. 18. The cross correlation function between set I.a and set II.a obtained by subtracting the respective average cross-section fits from the data in set I and set II. The cross-section data have been averaged over neutron energy intervals 400-eV wide.

TABLE VIII. Parameters for the intermediate structure in the ^{238}U neutron capture cross section between 5 keV and 100 keV (set I).

Doorway no.	E_μ (keV)	$\Gamma_{\mu n}$[a] (keV)	$\Gamma^{(0)}_{\mu n}$[a,b] (eV)	$U_{\mu n}$[a] (eV)	$K_{\mu n}$[a] (eV)	$I_{\mu n}$[a] $(eV)^2$	$J_{\mu n}$[a] $(eV)^2$
1	13.8	1.05	8.9	6.02	−0.06	272	−4.4
2	20.0	116.3	822.3	1.54	2.90	58	225.6
3	30.0	25.6	147.8	4.14	2.52	113	162.0
4	37.0	0.71	3.7	10.05	1.66	309	104.0
5	44.0	22.8	108.5	4.66	0.19	104	9.3
6	50	24.7	110.5	4.17	−0.51	100	9.7
7	54.0	27.3	117.3	4.15	0.83	91.0	6.05
8	61.0	19.3	78.2	3.84	0.329	101.0	−12.62
9	78	3.85	13.8	1.99	1.71	59	128

[a] See text for the definitions of this parameter.
[b] Reduced neutron widths for the doorway states, $\Gamma^{(0)}_{\mu n} = E_\mu^{1/2}\Gamma_{\mu n}$.

an intermediate structure in the ^{238}U neutron capture cross section.

VII. INTERPRETATION OF THE ^{238}U NEUTRON CAPTURE CROSS SECTION IN TERMS OF A MODULATED STRENGTH FUNCTION

The average cross-section fit discussed in Sec. III is related only to the smooth energy dependence of the cross section. In order to describe the local enhancement of the cross section at particular neutron energies, we have fitted the neutron capture cross section of set I with the functional relation given by Eq. (5) which includes the generalized strength function defined by Eq. (7). To implement the fitting procedure, we have arbitrarily assigned $J = \frac{1}{2}$ and $l = 1$ to all the doorway states. Also we have assumed that the entrance doorway states have zero radiation and fission widths (i.e., $\Gamma_\mu = \Gamma_{\mu n}$). The fit obtained for set I, averaged over 400-eV energy intervals, is shown in Fig. 19.

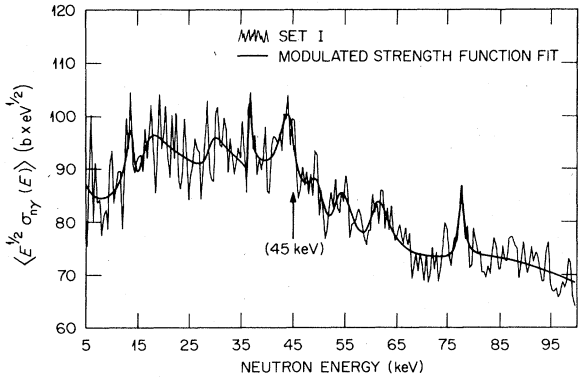

FIG. 19. Modulated strength function fit to the ^{238}U neutron capture cross section, set I. The cross-section data have been averaged over neutron energy intervals 400-eV wide.

The fit with the modulated strength function was then utilized as the reference line for the Wald-Wolfowitz runs test. The value of the ratio ϵ_R obtained in this case was 0.25 which is roughly a factor of ten smaller than that corresponding to the same test performed on the basis of the usual average cross-section fit.

The autocorrelation function for set I, after subtraction of the intermediate structure fit, is shown in Fig. 20. For energy shifts above 3 keV, the autocorrelation function is practically zero which is in fact an indication of the "goodness" of the fit to the data in the entire correlation range with the exception of the structure left around 65 keV.

The set of parameters arising from the modulated strength function fit is shown in Table VIII. This fit is nonunique mainly for two reasons:

(i) It is not clear how to distinguish between local enhancements of the cross section due to the arbitrarily picked doorway states and to the statistical fluctuations of the nuclear resonance parameters, because the statistical tests give only "global" criteria for intermediate structure.

(ii) The spin and parity of the doorway states has been arbitrarily assigned.

In view of these restrictions the usefulness of the fit lies in that it provides a much more accurate description of the cross section than the usual average cross-section fit. This is of interest in the calculation of neutron reaction rates. In addition one can also derive some general physical information from the study of the modulated strength function fit.

We can explain the observed intermediate structure in the ^{238}U capture cross section by postulating doorway states with an average level

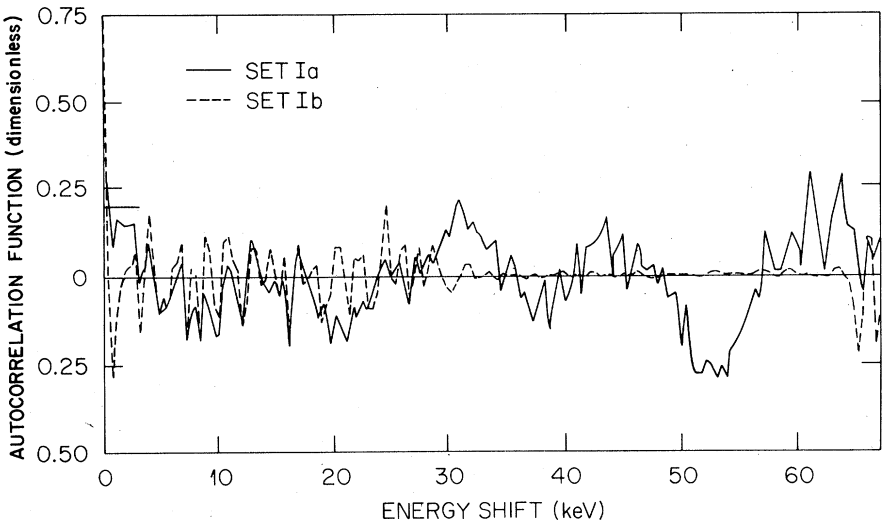

FIG. 20. The autocorrelation functions for set I.a and set I.b. The data set I.a are obtained by subtracting the average cross section from set I. The data set I.b are obtained by subtracting the modulated strength function fit from set I. The cross-section data have been averaged over neutron energy intervals 400-eV wide.

spacing of roughly 8 keV and escape widths to the continuum a few keV wide. The fact that the parameters $I_{\mu n}$ are always positive suggests that internal mixing predominates over external mixing. Both mixing effects appear strongly correlated as indicated by the values of the parameter $J_{\mu n}$. This situation is confirmed by the substantial amount of asymmetry exhibited by the intermediate structure lines (see Fig. 11). The widths of the doorway states fluctuate between 1 keV and 100 keV with an average of 27 keV, which is a small fraction of the Wigner limit of 0.6 MeV.

Since we cannot prove that the doorway states resulting from our fit constitute the only possible representation of the observed fluctuations, any conclusion based on the properties of these doorway states must be regarded as tentative. Thus it is possible that another set of doorway states with different properties could represent the cross section just as accurately.

VIII. DISCUSSION AND CONCLUSIONS

From the study of the Wald-Wolfowitz runs test applied to mockup cross sections, we confirm James' evaluation[38] of this test as suitable for the detection of intermediate structure in neutron cross sections. Care has to be exercised in the construction of the "reference" line for the implementation of this test. This line should represent accurately the long-range average behavior of the data in a physical sense so that one can separate out the fluctuations in an appropriate manner. For instance, a polynomial fit to the data points, besides being devoid of physical significance, could include some of the strength function modulation into the average behavior of the cross section.

The suitability of the reference line fit should be checked by the fitting of the experimental data "smoothed out" to the point in which all traces of intermediate structure have been erased. (See Fig. 4.)

The sensitivity of the runs test to the nature of the reference line is illustrated by the results shown in Table IX. These results show an increase in ϵ_R of more than a factor of four arising from an incomplete description of the physics involved in the average behavior of the capture cross section. Clearly, the runs test should be sensitive to "bad" fits, and it is. This suggests the possibility of utilizing this test as an added constraint to least square fitting procedures.

The main idea of the use of the cross correlation function to detect intermediate structure is the comparison of the correlation range of various sets of data. From the work in Sec. V on simulated cross sections, we have learned that in the neutron

TABLE IX. Comparison of the results of the Wald-Wolfowitz runs test for various fits of the ^{238}U neutron capture cross section for data set I averaged over 400-eV intervals.

	ϵ_R	$P(\epsilon_R)$ (%)
Set I	2.81	0.2
Set I.b[a]	9.23	$<10^{-15}$
Set I.c[b]	9.89	$<10^{-15}$

[a] Simultaneous fit to the ^{238}U neutron capture and inelastic cross sections without the threshold anomaly.

[b] Fit to the ^{238}U neutron capture only without the threshold anomaly.

energy range between 5 keV and 0.1 MeV, the autocorrelation function is made up of two components: (i) a smooth component with a correlation range of about 40 keV, and (ii) a second component exhibiting a pattern of peaks which only appear for the simulated cross sections with the intermediate structure.

The first component is related to the smooth energy dependence of the neutron penetration coefficients and disappears upon subtraction of the average cross-section fit. In regard to the second component, we know of its relation to the intermediate structure but have not established a quantitative, functional relationship between the latter and the observed correlation peaks.

In consequence the correlation function test is so far only a qualitative test. Nevertheless, as in the case of the Wald-Wolfowitz runs test, it appears to be sensitive to the presence of intermediate structure.

In constructing the reference line for the capture cross section we have found what seems to be a reasonable instance of a cusp anomaly in the form of a rounded step[13] (see Fig. 3). Attempts to fit the average cross section without the cusp effects (see Table IX) clearly illustrate the necessity to include such a threshold anomaly. Unfortunately, this feature introduces more adjustable parameters into the average cross-section fit. The $\{a_l\}$ and $\{b_l\}$ sets of parameters describing the threshold anomaly in both the capture and inelastic cross sections are related by the unitarity of the collision matrix, a constraint, which has been only partially fulfilled by the simultaneous fit of the capture and inelastic data. These considerations point towards the necessity of striving for the preservation of unitarity in the evaluation of the average parameters for the cross section calculations which are utilized in the computation of neutron reaction rates.

We have discussed the nonuniqueness of the fit to the observed structure in the ^{238}U neutron capture cross section: One can attach only a limited credibility to the parameters obtained for the doorway states which are responsible for the intermediate structure.

From the present study we draw the following conclusions:

(i) Autocorrelation function tests, as well as the Wald-Wolfowitz runs test, are suitable tools for the detection of intermediate structure.

(ii) The comparison of the above statistical tests as applied on mockup cross sections and experimental data indicates with a confidence limit, corresponding to about 3 standard deviations for a normal distribution, that the observed structure does not arise only from the statistical fluctuations of the nuclear resonance parameters.

(iii) A threshold anomaly in the form of a rounded step at the opening of the inelastic channel (2+ state at 45 keV) has been found and interpreted in the ^{238}U neutron capture cross section.

ACKNOWLEDGMENTS

The authors are grateful to N. Hill, R. W. Ingle, and H. Weaver for their help and advice in the collection and evaluation of the experimental data, to R. W. Peelle for many discussions in connection with this work, and to R. Q. Wright for providing an evaluated inelastic scattering cross section. This work was supported by the Reactor Research and Technology Division, Reactor Design, Department of Energy, under Contract No. W-7405-eng-26 with the Union Carbide Corporation.

APPENDIX A: PARAMETERS FOR THE AVERAGE CROSS-SECTION CALCULATION AND THE DEFINITION OF THE CORRELATION FUNCTION

The neutron widths are given in the usual form

$$\Gamma_{\lambda n}^{(l)} = \left(\frac{E_L}{E_r}\right)^{1/2} V_l \Gamma_{0\lambda n}^{(l)} \tag{A1}$$

where E_L is the laboratory energy of the neutron and E_r is the reference energy (usually taken as 1 eV), $\Gamma_{0\lambda n}^{(l)}$ are the reduced neutron widths and

$$V_0 = 1, \tag{A2}$$

$$V_1 = \rho^2/(1+\rho^2), \tag{A3}$$

$$V_2 = \rho^4/(9+3\rho^2+\rho^4), \tag{A4}$$

with

$$\rho = ka, \tag{A5}$$

$$k = \left(\frac{2M_n}{\hbar^2} E\right)^{1/2} = 2.19\times 10^9 E_L{}^{1/2}\ \text{cm}^{-1} \tag{A6}$$

where E_L is given in electron volts and M_n is the reduced mass in the neutron channel. The channel radius, a, is computed according to the ENDF/B (Ref. 17) prescription:

$$a = (1.23A^{1/3} + 0.8)10^{-13}\ \text{cm}, \tag{A7}$$

where A is the nucleus mass number. In the present case, one obtains

$$a = 0.842\times 10^{-12}\ \text{cm}.$$

The neutron inelastic widths $\Gamma_{\lambda n}^{(l)}$, are given by Eq. (A1) with the penetration coefficients V_l computed by Eq. (A2) and (A3) with

$$\rho' = 2.19\times 10^9 (E - E_c)^{1/2} a. \tag{A8}$$

The average radiation width $\langle\Gamma_\gamma\rangle$ was taken to be the same (0.0235 eV) for all spins and parities.[39]

For the average cross-section calculations, the statistical fluctuations factor $R_l^{n\gamma}$ was obtained from the expression[18]

$$R_l^{n\gamma} = \frac{\langle\Gamma_\lambda\rangle}{\langle\Gamma_n\rangle}\int d\Gamma_{\lambda n}\left(\frac{\Gamma_{\gamma n}}{\Gamma_\lambda}\right)P_2'(\nu_n,\Gamma_{\lambda n}), \tag{A9}$$

where $P_2'(\nu_n,\Gamma_{\lambda n})$ is the χ^2 distribution with ν_n degrees of freedom. For $\nu_n=1$ Eq. (A9) becomes

$$R_l^{n\gamma} = (1+2b_l)(1-2b_l^{1/2}Y_l) \tag{A10}$$

with

$$Y_l = 1-\phi(b_l)/\phi'(b_l), \tag{A11}$$

where

$$b_l = \langle\Gamma_\gamma\rangle/2\langle\Gamma_{\lambda n}\rangle \tag{A12}$$

and $\phi(b_l)$, $\phi'(b_l)$ are the error function and its derivative, respectively. The fluctuation factor $R_l^{nn'\gamma}$ for the average neutron inelastic cross section was taken to be unity.[18] For any values of the angular momentum l the statistical fluctuation factors $R_{1_{l_1}}$ and $R_{2_{l_2}}$ are defined by the relations

$$R_1 = \frac{\langle\Gamma_\lambda\rangle+\langle\phi_\lambda\rangle}{\langle\Gamma_{\lambda n}\rangle\langle\Gamma_{\lambda\gamma}\rangle}\int d\Gamma_{\lambda n}\,d\Gamma_{\lambda\gamma}\,d\phi_\lambda \times\left(\frac{\Gamma_\lambda\Gamma_{\lambda\gamma}}{\Gamma_\lambda+\phi_\lambda}\right)P_1(\Gamma_{\lambda n},\Gamma_{\lambda\gamma},\phi_\lambda), \tag{A13}$$

$$R_2 = \frac{\langle\Gamma_\lambda\rangle+\langle\phi_\lambda\rangle}{\langle\Gamma_{\lambda n}\rangle\langle\theta_{\lambda n}\rangle}\int d\Gamma_{\lambda n}\,d\phi_\lambda\,d\theta_{\lambda n} \times\left(\frac{\Gamma_{\lambda n}\theta_{\lambda n}}{\Gamma_\lambda+\Phi_\lambda}\right)P_2(\Gamma_{\lambda n},\Phi_\lambda,\theta_{\lambda n}). \tag{A14}$$

The probability distribution functions P_1 and P_2 are not known, although in principle they could be calculated by Monte Carlo techniques. Nevertheless, this is not felt necessary since the modulated part of the total width, i.e. ϕ_λ, is smaller than $\langle\Gamma_\gamma\rangle$. Hence we can rewrite Eq. (A13) and (A14) in the form

$$R_1 = \frac{\langle\Gamma_\lambda\rangle}{\langle\Gamma_{\lambda n}\rangle\langle\Gamma_{\lambda\gamma}\rangle}\int d\Gamma_{\lambda n}\,d\Gamma_\gamma\left(\frac{\Gamma_{\lambda n}\Gamma_{\lambda\gamma}}{\Gamma_\lambda}\right)P_1'(\Gamma_{\lambda n},\Gamma_{\lambda\gamma}), \tag{A15}$$

$$R_2 = \frac{\langle\Gamma_\lambda\rangle}{\langle\Gamma_{\lambda n}\rangle}\int d\Gamma_{\lambda n}\left(\frac{\Gamma_{\lambda n}}{\Gamma_\lambda}\right)P_2'(\nu_n,\Gamma_{\lambda n}), \tag{A16}$$

where we have neglected the fluctuations in $\theta_{\lambda n}$.

Next, on the assumption that the radiation and neutron widths are not correlated, we write

$$P_1'(\Gamma_{\lambda n},\Gamma_{\lambda\gamma}) = P_2'(\nu_n,\Gamma_{\lambda n})P_\gamma(\nu_\gamma,\Gamma_{\lambda\gamma}), \tag{A17}$$

where $P_\gamma(\nu_\gamma,\Gamma_{\lambda\gamma})$ is the χ^2 distribution for the radiation widths and ν_γ the number of degrees of freedom. By taking everywhere $\Gamma_{\lambda\gamma}$ equal to the average value, $\langle\Gamma_\gamma\rangle$, ν_γ becomes very large and it is easily seen from Eqs. (A17), (A16), and (A15) that $R_1=R_2$. Hence within the above approximations we can compute the statistical fluctuation factors R_1 and R_2 from Eq. (A10).

Given two ordered sets of objects, $\{X_i\}$ and $\{Y_i\}$ $(i=1,2,\ldots,N)$, with the average values $\langle X\rangle$ and $\langle Y\rangle$, one defines the normalized cross correlation function as

$$C_{XY}(j) = \mathrm{cov}(X_i,Y_{i+j})/[\mathrm{var}(X_i)\,\mathrm{var}(Y_i)]^{1/2}, \tag{A18}$$

where the covariance between $\{X_i\}$ and $\{Y_i\}$ is given by

$$\mathrm{cov}(X_i,Y_{i+j}) = \sum_{i=1}^{N}(X_i-\langle X\rangle)(Y_{i+j}-\langle Y\rangle). \tag{A19}$$

[1] G. de Saussure *et al.*, Nucl. Sci. Eng. 51, 385 (1973).

[2] R. R. Spencer and F. Käppeler, in *Proceedings of the Conference on Nuclear Cross Sections and Technology, Washington, D. C., March 3–7, 1975*, edited by R. C. Schrack and C. D. Bowman (National Bureau of Standards Special Publication No. 425, 1975), Vol. II, p.620.

[3] D. Kopsch, S. Cierjacks, and G. J. Kirouac, in *Proceedings of the Second International Atomic Energy Conference on Nuclear Data for Reactors, Helsinki, Finland, 1970* (IAEA, Vienna, 1971), Vol. II.

[4] J. Jary, Ch. Lagrange, and P. Thomet, in Proceedings of the National Soviet Conference on Neutron Physics, Kiev, 1975 (unpublished).

[5] A. Wald and J. Wolfowitz, Math. Stat. XI, No. 2 (1940); also *Documenta Geigy, Scientific Tables*, edited by K. Diem (Geigy Pharmaceuticals, Ardsley, New York, 1963).

[6] R. B. Perez, G. de Saussure, and M. N. Moore, in *Proceedings of the Second International Atomic Energy Symposium on Physics and Chemistry of Fission, Vienna, Austria, 1969* (IAEA; Vienna, Austria, 1969).

[7] H. Feshback, Rev. Mod. Phys. 46, 1 (1974), and in *Proceedings of the International Conference on Nuclear Physics*, Munich, 1973, edited by J. de Boer and H. J. Mang (North-Holland, Amsterdam/American Elsevier, New York, 1973). See also B. Block and H. Feshbach Ann. Phys. (N.Y.) 23, 47 (163).

[8] H. Feshbach and E. Sheldon, Phys. Today 30, (No. 2) 40 (1977).

[9] R. B. Perez, G. de Saussure, D. K. Olsen, and F. C.

Difillippo, Phys. Rev. C 17, 964 (1978). (A slightly different notation has been used in the present paper in regard to the parameters of the doorway states.)
[10]G. D. James, Nucl. Phys. A170, 309 (1971).
[11]R. L. Macklin, Nucl. Instrum. Methods 91, 79 (1971).
[12]R. L. Macklin and N. W. Hill, Nucl. Instrum. Methods 96, 509 (1971).
[13]R. G. Newton, *Scattering Theory of Waves and Particles* (McGraw-Hill, New York, 1966), p. 533.
[14]E. P. Wigner, Phys. Rev. 73, 1002 (1948).
[15]W. H. Guier and R. W. Hart, Phys. Rev. 106, 296 (1957).
[16]Private communication from R. Q. Wright (1978). These values are based on an unpublished evaluation by A. B. Smith, proposed for the Evaluated Nuclear Data File ENDF/B-V.
[17]M. D. Drake, BNL Report No. 50274 (T-601), Vol. I, 1970 (unpublished); see also Report No. BNL-NCS-50496, revised by D. Garber, C. Dunford, and S. Pearlstein, 1975 and 1976 (unpublished).
[18]J. J. Schmidt, KFK 120, Report No. EANDC-E-35U, 1966 (unpublished), pp. B43, B48.
[19]H. Feshback, A. K. Kerman, and R. H. Lemmer, Ann. Phys. (N.Y.) 41, 230 (1967).
[20]A. M. Lane, in *Isospin in Nuclear Physics*, edited by D. H. Wilkinson (North-Holland, Amsterdam, 1969), p. 511.
[21]D. Robson, in *Isospin in Nuclear Physics*, edited by D. H. Wilkinson (North-Holland, Amsterdam, 1969), p. 463.
[22]D. Robson, Phys. Rev. 137, B535 (1965).
[23]V. M. Strutinsky, Nucl. Phys. A95, 420 (1967).
[24]H. Weigmann, Z. Phys. 214, 7 (1968).
[25]J. E. Lynn, U. K. Atomic Energy Authority, Harwell, Report No. AERE-R5891, 1968 (unpublished).
[26]R. C. Block, R. W. Hockenbury, R. E. Slovacek, E. B. Bean, and D. S. Cramer, Phys. Rev. Lett. 31, 247 (1973).
[27]J. Blons, C. Mazur, and D. Paya, *Proceedings of the Conference on Nuclear Cross Sections and Technology, Washington, D. C., March 3–7, 1975,* edited by R. A. Schrack and C. D. Bowman (National Bureau of Standards Special Publication No. 425, 1975), Vol. II, p. 642.
[28]F. C. Difilippo, R. B. Perez, G. de Saussure, D. K. Olsen, and R. W. Ingle, Trans. Am. Nucl. Soc. 23, 499 (1976). Also, Nucl. Sci. Eng. 63, 153 (1977).
[29]R. E. Slovacek, D. S. Cramer, E. B. Bean, J. R. Valentine, R. W. Hockenbury, and R. C. Block, Nucl. Sci. Eng. 62, 455 (1977).
[30]G. D. James, G. de Saussure, and R. B. Perez, Trans. Am. Nucl. Soc. 17, 495 (1973). See also R. B. Perez and G. de Saussure, in *Proceedings of the Conference on Nuclear Cross Sections and Technology, Washington, D.C., March 3–7, 1975,* edited by R. A. Schrack and C. D. Bowman (National Bureau of Standards Special Publication No. 425, 1975), Vol. I, p. 623.
[31]M. S. Moore, *Statistical Properties of Nuclei*, edited by J. B. Garg (Plenum, New York, 1972), p. 55.
[32]Y. Baudinet-Robinet and C. Mahaux, Phys. Rev. C 9, 723 (1974).
[33]G. de Saussure and R. B. Perez, Nucl. Sci. Eng. 52, 382 (1973).
[34]F. C. Difilippo and R. B. Perez, Report No. ORNL/TM-5850, 1977 (unpublished).
[35]G. de Saussure and R. B. Perez, Report No. ORNL-TM-2599, 1969 (unpublished).
[36]C. E. Porter and R. G. Thomas, Phys. Rev. 104, 483 (1956).
[37]E. P. Wigner, in *Statistical Theory of Spectra Fluctuations*, edited by C. E. Porter (Academic, New York, 1965), p. 120.
[38]G. D. James, Report No. ANL-76-90, 1976 (unpublished), p. 382.
[39]G. de Saussure, D. K. Olsen, R. B. Perez, and F. C. Difilippo, in *Progress in Nuclear Energy* (Pergamon, London, 1979), Vol. 3, pp. 87–124.